Inorganica Chimica Acta, 160 (1989) 123–134

Synthetic Analogue Approach to Cobalt(III)–Bleomycin: Synthesis, Crystal and Solution Structures and Redox Properties of Bis(*N*-(2-(4-imidazolyl)ethyl)pyrimidine-4-carboxamido)cobalt(III) Perchlorate·2.25H_2O

MARK MUETTERTIES, PRADIP K. MASCHARAK*

Department of Chemistry, Thimann Laboratories, University of California, Santa Cruz, CA 95064 (U.S.A.)

MARY B. COX and SATISH K. ARORA

Drug Dynamics Institute, College of Pharmacy, University of Texas, Austin, TX 78712 (U.S.A.)

(Received October 5, 1988)

Abstract

Aerobic oxidation of mixtures of PrpepH (**3**), a peptide ligand that contains three of the five proposed donor centers of the metal-chelating portion of the antitumor drug bleomycin (BLM) and cobalt(II) salts (ratio 2:1) in water or methanol affords the cobalt(III) complex $[Co(Prpep)_2]^+$ which has been isolated as the perchlorate and the tetrafluoroborate salt. $[Co(Prpep)_2]ClO_4 \cdot 2.25H_2O$ (**5a**) crystallizes in the orthorhombic space group *Pbca* with $a = 14.553(5)$, $b = 16.765(7)$, $c = 21.745(8)$ Å and $Z = 8$. The structure was refined to $R = 6.2\%$ by using 3273 unique data ($F_o^2 > 2.5\sigma(F_o^2)$). The coordination geometry around low-spin Co(III) is octahedral with Co–N(pyrimidine) = 1.943(5), Co–N(imidazole) = 1.931(5) and Co–N(amido) = 1.927(5) Å, respectively. The complex is isolated as the *mer* isomer. On reduction, $[Co(Prpep)_2]^+$ yields a cobalt(II) species that rapidly decomposes in solution. The solution structure of $[Co(Prpep)_2]^+$ has been explored with the aid of one- and two-dimensional ^1H and ^{13}C NMR spectroscopy.

Introduction

Since the metal-ion-promoted DNA cleavage property of bleomycins (BLM, **1**), a family of glycopeptide antitumor antibiotics, is believed to be responsible for the drug action, the coordination chemistry of metallobleomycins (M–BLMs) and their interaction with DNA have been studied quite extensively [1–7]. Despite direct DNA cleavage activity [8], the coordination chemistry of cobalt–BLM chelates has been explored [1–7, 9–15] and Co–BLMs have found use in specific clinical applications. For example, kinetically inert $^{57}Co(III)$–BLMs accumulate selectively in the nuclei of certain types of cancer cells and hence are used as diagnostic agents in nuclear medicine [14]. The recent report that Co(III)–BLM can cause DNA strand breaks following photoreduction by UV or visible light [16] has stimulated renewed interest in the chemistry of Co(III)–BLM and its interaction with DNA under illumination. As part of a systematic synthetic analogue approach [17] to M–BLMs, we have recently reported [18] the structure and properties of a Co(III) complex $[Co(Pypep)_2]ClO_4 \cdot H_2O$ (**4**) of a peptide ligand namely, *N*-(2-(4-imidazolyl)ethyl)-pyridine-2-carboxamide (**2**, PypepH). Since BLM contains a pyrimidine and not a pyridine ring in the metal-chelating locus of the drug, we have altered **2** accordingly and have synthesized *N*-(2-(4-imidazolyl)-ethyl)pyrimidine-4-carboxamide (**3**) as our new tailored fragment of BLM. This ligand contains three of the five proposed donor groups of BLM (boxed area in **1**). Keeping up with our nomenclature, **3** is abbreviated as PrpepH; the dissociable H is the amide H. In this paper, we report the synthesis, spectral properties and the structure of a Co(III) complex of **3** of the formula $[Co(Prpep)_2]ClO_4 \cdot 2.25H_2O$ (**5a**)*. The solution structure of this synthetic analogue of Co(III)–BLM has also been established by two-dimensional NMR work. The complex **5a** provides important structural and spectroscopic parameters pertinent to Co(III)–BLM.

Experimental

Preparation of Compounds

Histamine (free base), 4-methylpyrimidine, selenium dioxide, lithium perchlorate, tetraethylam-

*Author to whom correspondence should be addressed.

*The other pyrimidine-based designed ligand namely, *N*-(2-(4-imidazolyl)ethyl)-2-methyl-5-bromopyrimidine-4-carboxamide (PmpepH) [19] does not form a 'bis' complex of the type $[Co(Pmpep)_2]^+$ presumably due to steric hindrance.

0020-1693/89/$3.50

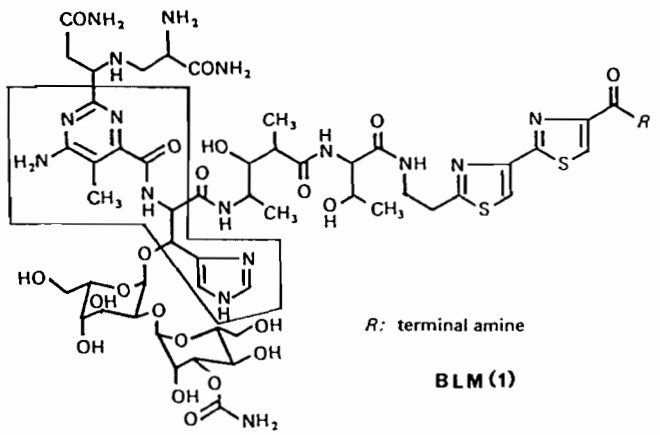

BLM (1)

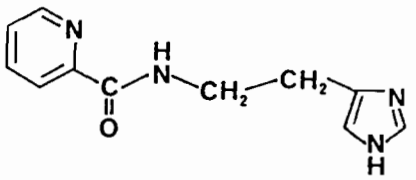

PypepH (2)

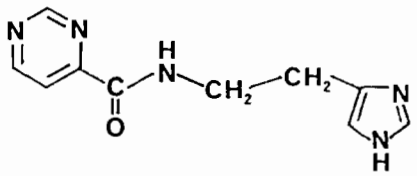

PrpepH (3)

monium tetrafluoroborate and cobalt(II) chloride hexahydrate were procured from Aldrich Chemical Company. Cobalt(II) acetate tetrahydrate was purchased from Alfa Products (Morton Thiokol Inc.).

PrpepH (3)

Conversion of 4-methylpyrimidine to 4-pyrimidinecarboxylic acid was completed according to a published procedure [20]. A batch of 16 g (0.13 mol) of the acid was dissolved (small amount of the acid remained undissolved) in 200 ml of anhydrous ethanol and dry HCl gas was bubbled through the brown mixture for 5 h*. The temperature was maintained at 55 °C. Following removal of ethanol, the brown oil was distilled *in vacuo* to collect 10 g (66 mmol, 51%) of ethyl-4-pyrimidinecarboxylate. Next, 7.4 g (66 mmol) of histamine were added to the ester dissolved in 200 ml of benzene and the mixture was heated to reflux for 10 h. The reaction mixture was then cooled (0 °C) and the light cream-colored solid was filtered. PrpepH thus obtained (12 g, 84%) was pure enough for syntheses of metal complexes. Recrystallization from methanol afforded off-white needles; melting point (m.p.) 196–197 °C. ^{1}H NMR (300 MHz, $(CD_3)_2SO$, 313 K); 2.82 (t, J = 7.2 Hz, 2H), 3.60 (q, J = 6.6 Hz, 2H), 6.87 (s, 1H, *Im* (imidazolyl C–H)), 7.58 (s, 1H, *Im*), 8.04 (d, J = 4.8 Hz, *Pm* (pyrimidine ring C–H)), 9.07 (d, J = 4.8 Hz, *Pm*), 9.10 (br, 1H, peptide NH), 9.32 (s, 1H, *Pm*), 11.15 (br, 1H, *Im* NH). Selected IR bands (KBr pellet, cm^{-1}): 3360(m), 3200(m), 3000(m), 1665-(ν_{CO}, s), 1520(s), 1430(s), 1270(m), 1200(m), 1080-(m), 970(w), 820(m), 760(s), 710(s), 665(s), 615(s), 480(w) and 410(m).

Anal. Calc. for $C_{10}H_{11}N_5O$: C, 55.27; H, 5.11; N, 32.25. Found: C, 55.40; H, 5.17; N, 32.34%.

[Co(Prpep)$_2$]ClO$_4$·2.25H$_2$O (5a)

A 450 mg (2 mmol) amount of Co(II) acetate tetrahydrate was dissolved in 30 ml of 1:1 vol./vol. mixture of water and methanol. The resulting pink solution was slowly added with stirring to a solution of 900 mg (4.15 mmol) of PrpepH in 30 ml of water. The mixture immediately turned deep red. After 30 min, a batch of 450 mg (4.3 mmol) of $LiClO_4$ in 5 ml water was added and the clear deep red solution was stored at 0 °C for 20 h. The dark red crystals were collected by filtration and dried in air. A batch of 750 mg (59%) of dark red blocks was obtained; m.p. 255–257 °C (dec.). Presence of water molecules was confirmed by X-ray crystallography and NMR spectroscopy (*vide infra*). When the reaction was performed in anhydrous methanol, dark red crystals (needles) of $[Co(Prpep)_2]ClO_4 \cdot CH_3OH$ were isolated in 52% yield. Presence of methanol in the crystals was revealed by NMR spectroscopy. Selected IR bands (KBr pellet, cm^{-1}): 3200(br, s), 2960(s), 1610(ν_{CO}, s), 1500(s), 1400(s), 1280(m), 1240(m), 1120(ν_{ClO_4}, vs), 840(m), 690(m), 630(m) and 510(w).

Anal. Calc. for $C_{20}H_{24.5}N_{10}O_{8.25}CoCl$: C, 38.05; H, 3.91; N, 22.18. Found: C, 37.90; H, 3.93; N, 21.98%.

The tetrafluoroborate salt $[Co(Prpep)_2]BF_4 \cdot 2H_2O$ (**5b**) was isolated from a reaction mixture of

*The reaction mixture became homogeneous within *c.* 2h.

TABLE 1. Summary of crystal data, intensity collection and structure refinement parameters for $[Co(Prpep)_2]ClO_4 \cdot 2.25H_2O$ (5a)

Formula (molecular weight)	$C_{20}H_{24.5}N_{10}O_{8.25}CoCl$ (631.37)
a (A)	14.553(5)
b (A)	16.765(7)
c (A)	21.745(8)
Crystal system	orthorhombic
V (A^3)	5305(3)
Z	8
D_{calc} (g/cm^3)	1.581
D_{obs} (g/cm^3)	1.60(1)[a]
Space group	*Pbca*
Crystal dimensions (mm)	0.23 × 0.32 × 0.63
Radiation	Mo Kα (λ = 0.71069 Å)
Absorption coefficient, μ (cm^{-1})	10.19
Scan speed (°/min)	3–6
2θ limit (°)	$4.0 < 2\theta < 55.0$
Scan range (°)	(ω) symmetrically over 1.0 about $K\alpha_{1,2}$ maximum
Background/scan time ratio	0.5
Transmission factor range	0.78–0.84
Data collected	6091 ($+h, +k, +l$)
Unique data ($F_o^2 > 2.5\sigma(F_o^2)$)	3273
No. variables	462
Goodness of fit	1.85
R[b] (%)	6.2
R_w[c] (%)	6.9
Temperature (K)	298
Largest Δ/σ in refinement	0.008
Maximum (e/Å^3)	0.81

[a]Determined by the neutral buoyancy technique in $CHCl_3/CHBr_3$. [b]$R = \Sigma||F_o| - |F_c||/\Sigma|F_o|$. [c]$R_w = [\Sigma w(|F_o| - |F_c|)^2/\Sigma w|F_o|^2]^{1/2}$; $w = 1/\sigma(|F_o|)^2$.

$Co(CH_3COO)_2 \cdot 4H_2O$ and PrpepH (ratio 1:2) in aqueous methanol following addition of Et_4NBF_4. The dark red blocks thus obtained were characterized by IR, NMR, and absorption spectroscopy.

Anal. Calc. for $C_{20}H_{24}N_{10}O_4CoBF_4$: C, 39.09; H, 3.94; N, 22.81. Found: C, 39.15; H, 3.89; N, 22.71%.

$[Co(Prpep)_2]^+$ from $CoCl_2 \cdot 6H_2O$

A solution of 238 mg (1 mmol) of cobalt(II) chloride hexahydrate in 5 ml of water was added with stirring to a solution of 450 mg (2.1 mmol) of PrpepH in 12 ml of 1:1 aqueous methanol. The color of the reaction mixture turned to deep red as the addition continued. After 30 min, a batch of 260 mg (2.5 mmol) of $LiClO_4$ in 3 ml of water was added and the deep red solution was stored at 0 °C for 15 h. Dark red needles of **5a** were isolated in 60% yield.

Physical Measurements

Infrared spectra were obtained with a Nicolet MX-S FTIR spectrometer. Absorption spectra were measured on a Perkin-Elmer Lambda 9 spectrophotometer. ^1H and ^{13}C NMR spectra were recorded on a General Electric 300 MHz GN-300 instrument. Samples were dissolved in $(CD_3)_2SO$ (99.5% D). Multiplicities of ^{13}C NMR peaks were determined from APT or DEPT data. Standard pulse sequences [21] were used to obtain $^1H-^1H$ and $^1H-^{13}C$ two-dimensional scalar correlated NMR spectra. Experimental detail has already been published [18]. Electrochemical measurements were performed with standard Princeton Applied Research instrumentation using a Pt or glassy carbon (GC) electrode; potentials were measured at ~25 °C versus a saturated calomel electrode (SCE) as reference. Elemental analyses were completed by Atlantic Microlab Inc., Atlanta, GA, U.S.A.

X-ray Data Collection and Reduction

Dark red blocks of $[Co(Prpep)_2ClO_4 \cdot 2.25H_2O$ (**5a**) were obtained by slow evaporation of an aqueous solution of the complex. Intensities were measured using Mo Kα radiation on a Syntex P2 diffractometer equipped with graphite monochromator. Table 1 summarizes the crystal data and data collection parameters. The orientation matrix and unit cell parameters were determined by using 24 machine-centered reflections in the region $15° < 2\theta < 30°$. Intensities of four check reflections were recorded every 96 reflections to monitor crystal and instru-

ment stability. The intensities were corrected for Lorentz and polarization effects and absorption.

Solution and Refinement of the Structure

The structure was solved by the direct-methods program SHELX [22] with $Es > 1.2$. The E map revealed atoms of the cation, anion and one water molecule. The structure was refined isotropically by least-squares method to an R value of 0.242. A difference Fourier map at this stage revealed another water molecule as well as the fact that the four oxygens of the perchlorate were disordered. The occupancy of the primary positions as well as secondary positions were refined with the total occupancy of the pair being kept at 1.0. The refined occupancies of the primary and secondary positions were 0.65 and 0.35, respectively. The R factor at this stage of refinement with isotropic thermal parameters had a value of 0.125. A difference Fourier map at this point further revealed a partial water molecule whose occupancy refined to 0.25. Continuing least-squares refinement with anisotropic thermal parameters for non-hydrogen atoms (except the partial water molecule) reduced R to 0.070. At this stage, all the hydrogen atoms belonging to the cation and the two fully occupied water molecules were located from the difference map and refined with isotropic thermal parameters to R value of 0.062. The refinement was based on F_o and the quantity minimized being $\Sigma w(F_o - F_c)^2$, where $w = 1/\sigma(F_o)^2$. A total of 3273 unique data ($F_o^2 > 2.5\sigma(F_o^2)$) was used in the refinement. Scattering factors for nonhydrogen and hydrogen atoms were taken from literature tabulations [23]. Atomic positional parameters are listed in Table 2. Selected bond distances and angles are presented in Table 3. See also 'Supplementary Material'.

Results and Discussion

Oxygenation of mixtures of cobalt(II) salts and the peptide ligand PrpepH (**3**) leads to formation of the cobalt(III) complex $[Co(Prpep)_2]^+$ which has been isolated both as the perchlorate (**5a**) and the tetrafluoroborate (**5b**) salt. Since coordination of the deprotonated amido N to cobalt appears to be a key step toward oxidation of the metal center, syntheses of the peptide complexes of tervalent cobalt are usually performed in basic (pH ~ 10) solutions [24–26]. In the present case however, no base is required to promote the deprotonation of the amide group of **3** in either aqueous or methanolic solution; $[Co(Prpep)_2]^+$ has been synthesized starting from both cobalt(II) acetate tetrahydrate and cobalt(II) chloride hexahydrate. The characteristic deep red color of $[Co(Prpep)_2]^+$ is observed immediately after cobalt(II) chloride and **3** (ratio 1:2.1) are mixed in water. The aerobic oxidation step is extremely rapid in water and no brown coloration due to oxygenated (superoxo or binuclear peroxo) intermediate(s) [27] is observed. That oxygen is the oxidizing agent in these syntheses has been confirmed by the facts that under strictly anaerobic conditions, the reaction mixture of 1 eq. of cobalt(II) acetate tetrahydrate and 2.1 eq. of **3** remains orange (*vide infra*) and changes to deep red only when exposed to air. When anhydrous cobalt(II) chloride is allowed to react with **3** (ratio 1:2.1) in anhydrous methanol, a brown coloration (indicating the formation of oxygenated complex) is observed; the mixture turns to deep red within a few minutes, however. Addition of $LiClO_4$ to the deep red solution affords crystals of **5a** in good yield. As reported earlier [18], formation of $[Co(Pypep)_2]^+$ requires the presence of a base in the reaction mixture; with PrpepH, no base is needed. Clean oxidation to Co(III) and formation of the desired 'bis' complexes of PypepH and PrpepH suggest that the deprotonated amido Ns stabilize tervalent cobalt and Co(III)–BLM is likely to contain amido N in the first coordination sphere of the metal.

Structure of $[Co(Prpep)_2]ClO_4 \cdot 2.25H_2O$ (5a)

The crystal structure of $[Co(Prpep)_2]ClO_4 \cdot 2.25H_2O$ (**5a**) consists of discrete cations, anions and water molecules of crystallization. The water molecules are involved in extensive hydrogen bonding. Selected hydrogen bonding distances include OW(1)–H--O(1) [2.736 Å], OW(1)–H--N(2) [2.821 Å], OW(2)–H--OW(1) [2.769 Å] and OW(2)–H--N(7) [2.805 Å]. An ORTEP drawing of the cation and the atom-labeling scheme is shown in Fig. 1. The cobalt(III) center is in an octahedral environment of six N donor centers of two tridentate anionic ligands. The coordinated pyrimidine and the imidazole N atoms of each ligand are *trans* to one another. The two deprotonated amido N atoms are also *trans* to one another. The complex is therefore the *mer* isomer. Both $[Fe(Pypep)_2]^+$ and $[Co(Pypep)_2]^+$ have been isolated as the *mer* isomer. Clearly, ligand frameworks of the type **2** and **3** prefer to coordinate in a plane and this in turn suggests that analogous portion of BLM (boxed are in **1**) is likely to be ligated to the metal ions in the basal plane.

Selected interatomic distances and angles for **5a** are listed in Table 3. The Co(III)–N_{pm} (pm = pyrimidine) distance (1.943(5) Å) is close to the average Co(III)–N_{pm} distance of 1.979(5) Å in the *fac* isomer of tris(4,6-dimethylpyrimidine-2-thionato)cobalt(III) [28]. In bis(acetylacetonato)(nitro)(2-aminopyrimidine)cobalt(III), where the pyrimidine ligand is monodentate, the Co(III)–N_{pm} distance is longer (2.019(7) Å) [29]. The Co(III)–N_{im} (im = imidazole) distance in **5a** (1.931(5) Å) is comparable to that observed in histidinato (His) complexes like $[Co(NO_2)(L\text{-}His)_2] \cdot H_2O$ (1.958(10) Å] [30] and [Co(en)Cl-

TABLE 2. Atomic coordinates ($\times 10^4$) and equivalent isotropic displacement parameters ($Å^2 \times 10^3$) for **5a**

Atom	*x*	*y*	*z*	*U*(eq)[a]
Co	75388(6)	19483(4)	66597(3)	27(1)
O(1)	6015(3)	1322(3)	8122(2)	54(2)
O(2)	9050(3)	853(3)	5377(2)	47(2)
N(1)	6914(3)	2704(3)	6136(2)	31(2)
N(2)	6472(4)	3384(4)	5345(3)	48(2)
N(3)	6568(3)	1984(3)	7263(2)	32(2)
N(4)	8063(3)	1190(3)	7239(2)	28(2)
N(5)	9209(4)	332(3)	7650(3)	48(2)
N(6)	8190(3)	2813(3)	7053(2)	30(2)
N(7)	8601(4)	3712(3)	7715(3)	44(2)
N(8)	8513(3)	1797(3)	6072(2)	30(2)
N(9)	6972(3)	1084(3)	6202(2)	31(2)
N(10)	5744(4)	264(4)	5880(3)	54(2)
C(1)	6302(5)	3273(4)	6334(3)	37(2)
C(2)	6028(5)	3691(5)	5838(4)	52(3)
C(3)	6992(5)	2796(4)	5529(3)	37(2)
C(4)	6008(6)	3329(5)	6982(3)	45(3)
C(5)	5774(5)	2532(5)	7256(3)	44(3)
C(6)	6607(4)	1440(4)	7714(3)	35(2)
C(7)	7494(5)	995(3)	7706(2)	31(2)
C(8)	7741(5)	449(4)	8142(3)	42(2)
C(9)	8607(6)	137(4)	8093(4)	52(3)
C(10)	8892(5)	852(4)	7236(3)	40(2)
C(11)	8794(4)	3316(4)	6765(3)	30(2)
C(12)	9056(5)	3887(4)	7172(3)	42(2)
C(13)	8088(4)	3063(4)	7630(3)	37(2)
C(14)	9117(5)	3168(4)	6128(3)	40(2)
C(15)	9339(5)	2289(4)	6019(3)	36(2)
C(16)	8457(5)	1139(4)	5721(3)	34(2)
C(17)	7528(5)	783(3)	5760(3)	34(2)
C(18)	7195(5)	208(4)	5357(3)	45(3)
C(19)	6285(6)	−24(4)	5429(4)	53(3)
C(20)	6124(5)	810(4)	6242(3)	43(3)
Cl	8682(2)	3027(1)	4221(1)	81(1)
O(3)[0.65]	4006(14)	3125(18)	1377(11)	71(7)
O(4)[0.65]	3116(17)	3667(16)	609(9)	86(7)
O(5)[0.65]	3440(16)	2291(13)	587(10)	137(10)
O(6)[0.65]	4595(9)	3164(8)	407(5)	119(6)
O(7)[0.35]	2560(13)	2793(13)	1019(8)	93(8)
O(8)[0.35]	3488(33)	3674(24)	482(20)	105(18)
O(9)[0.35]	3938(36)	2917(35)	1404(19)	98(15)
O(10)[0.35]	3707(33)	2363(22)	440(14)	129(18)
OW(1)	10866(3)	767(3)	5699(2)	43(2)
OW(2)	3697(4)	771(3)	1060(2)	67(2)
OW(3)[0.25]	6560(10)	3280(9)	8832(7)	50

The numbers in brackets give the refined occupancy factors. Parameters for the cobalt atom were multiplied by 10^5. [a]Equivalent isotropic *U* defined as one third of the trace of the orthogonalized U_{ij} tensor.

(His)]Cl (1.946(3) Å) [31]. The Co(III)–N(amido) bond in **5a** is 1.927(5) Å long. Very similar lengths for the Co(III)–N(amido) bond have been reported with $(NH_4)[Co(gly\text{-}gly)_2]\cdot 2H_2O$ (1.92 Å) [32], $[Co(H_2O)_6][Co(gly\text{-}gly)_2]_2\cdot 12H_2O$ (1.87 Å) [33] and $[Co(NH_3)_2(L\text{-}ala\text{-}gly\text{-}gly)]$ (1.869(6) Å) [34]. For the sake of comparison, in $[Co(Pypep)_2]^+$ [18], the Co(III)–N_{py} (py = pyridine), Co(III)–N_{im} and Co(III)–N(amido) bond lengths are 1.937(5), 1.952(5), and 1.933(3) Å, respectively. In **5a**, significant deviation from 90° is observed with N(amido)–Co–N_{pm} angles (ave. 82.6(2)°) presumably due to formation of five-membered chelate rings with extended conjugation. Similar shortening of N(amido)–Co–N_{py} angles (ave. 83.3(2)°) has been observed with $[Co(Pypep)_2]^+$ [18]. Thus the dimensions of the $Co(III)N_6$ chromophore in $[Co(Prpep)_2]^+$ and $[Co(Pypep)_2]^+$ are quite similar.

TABLE 3. Selected bond distances and angles in $[Co(Prpep)_2]^+$

Distances (Å)			
Co–N(1)	1.931(5)	N(7)–C(12)	1.386(8)
Co–N(3)	1.929(5)	N(7)–C(13)	1.332(8)
Co–N(4)	1.945(5)	N(8)–C(15)	1.463(8)
Co–N(6)	1.931(5)	N(8)–C(16)	1.343(7)
Co–N(8)	1.926(5)	N(9)–C(17)	1.354(7)
Co–N(9)	1.942(5)	N(9)–C(20)	1.320(8)
O(1)–C(6)	1.253(7)	N(10)–C(19)	1.347(9)
O(2)–C(16)	1.238(7)	N(10)–C(20)	1.327(8)
N(1)–C(1)	1.374(7)	C(1)–C(2)	1.347(9)
N(1)–C(3)	1.334(8)	C(1)–C(4)	1.475(9)
N(2)–C(2)	1.355(9)	C(4)–C(5)	1.503(10)
N(2)–C(3)	1.305(8)	C(6)–C(7)	1.490(9)
N(3)–C(5)	1.476(8)	C(7)–C(8)	1.367(8)
N(3)–C(6)	1.341(7)	C(8)–C(9)	1.369(9)
N(4)–C(7)	1.351(7)	C(11)–C(12)	1.358(9)
N(4)–C(10)	1.333(8)	C(11)–C(14)	1.483(9)
N(5)–C(9)	1.343(9)	C(14)–C(15)	1.527(9)
N(5)–C(10)	1.335(8)	C(16)–C(17)	1.480(9)
N(6)–C(11)	1.370(7)	C(17)–C(18)	1.389(8)
N(6)–C(13)	1.332(7)	C(18)–C(19)	1.388(10)
Angles (°)			
N(3)–Co–N(1)	92.0(2)	C(20)–N(9)–C(17)	118.4(6)
N(4)–Co–N(1)	174.4(2)	C(20)–N(10)–C(19)	115.8(7)
N(4)–Co–N(3)	82.4(2)	C(2)–C(1)–N(1)	107.6(6)
N(6)–Co–N(1)	90.0(2)	C(4)–C(1)–N(1)	122.1(6)
N(6)–Co–N(3)	92.1(2)	C(4)–C(1)–C(2)	130.2(6)
N(6)–Co–N(4)	90.7(2)	C(1)–C(2)–N(2)	107.2(6)
N(8)–Co–N(1)	92.4(2)	N(2)–C(3)–N(1)	110.0(6)
N(8)–Co–N(3)	174.1(2)	C(5)–C(4)–C(1)	112.7(6)
N(8)–Co–N(4)	93.1(2)	C(4)–C(5)–N(3)	112.4(6)
N(8)–Co–N(6)	91.8(2)	N(3)–C(6)–O(1)	126.7(6)
N(9)–Co–N(1)	89.3(2)	C(7)–C(6)–O(1)	121.6(6)
N(9)–Co–N(3)	93.4(2)	C(7)–C(6)–N(3)	111.6(5)
N(9)–Co–N(4)	90.6(2)	C(6)–C(7)–N(4)	114.8(5)
N(9)–Co–N(6)	174.5(2)	C(8)–C(7)–N(4)	121.5(6)
N(9)–Co–N(8)	82.8(2)	C(8)–C(7)–C(6)	123.7(6)
C(1)–N(1)–Co	125.2(4)	C(9)–C(8)–C(7)	116.4(7)
C(3)–N(1)–Co	128.2(5)	C(8)–C(9)–N(5)	124.3(7)
C(3)–N(1)–C(1)	106.6(5)	N(5)–C(10)–N(4)	126.0(6)
C(3)–N(2)–C(2)	108.7(6)	C(12)–C(11)–N(6)	108.4(6)
C(5)–N(3)–Co	125.8(4)	C(14)–C(11)–N(6)	121.8(5)
C(6)–N(3)–Co	116.5(4)	C(14)–C(11)–C(12)	129.6(6)
C(6)–N(3)–C(5)	117.7(5)	C(11)–C(12)–N(7)	105.8(6)
C(7)–N(4)–Co	113.8(4)	N(7)–C(13)–N(6)	109.0(6)
C(10)–N(4)–Co	129.1(4)	C(15)–C(14)–C(11)	112.0(6)
C(10)–N(4)–C(7)	117.1(5)	C(14)–C(15)–N(8)	111.0(5)
C(10)–N(5)–C(9)	114.7(6)	N(8)–C(16)–O(2)	128.2(6)
C(11)–N(6)–Co	125.1(4)	C(17)–C(16)–O(2)	121.0(6)
C(13)–N(6)–Co	126.8(5)	C(17)–C(16)–N(8)	110.7(6)
C(13)–N(6)–C(11)	107.9(5)	C(16)–C(17)–N(9)	115.8(5)
C(13)–N(7)–C(12)	108.8(6)	C(18)–C(17)–N(9)	119.8(7)
C(15)–N(8)–Co	125.6(4)	C(18)–C(17)–C(16)	124.3(6)
C(16)–N(8)–Co	116.1(4)	C(19)–C(18)–C(17)	117.2(7)
C(16)–N(8)–C(15)	117.9(5)	C(18)–C(19)–N(10)	122.6(7)
C(17)–N(9)–Co	112.8(4)	N(10)–C(20)–N(9)	126.2(7)
C(20)–N(9)–Co	128.6(5)		

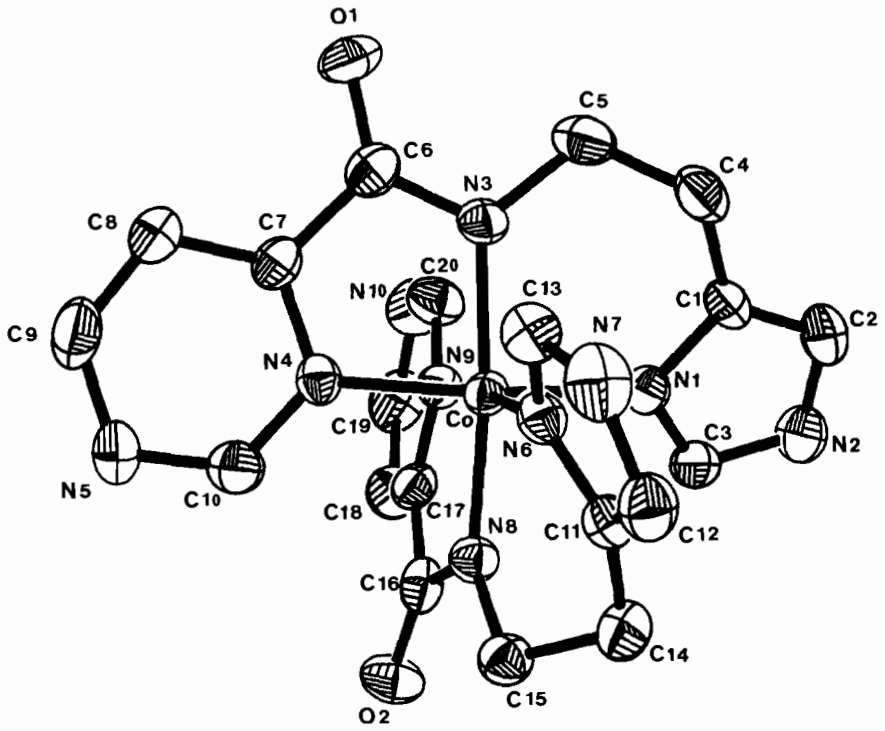

Fig. 1. ORTEP drawing of $[Co(Prpep)_2]^+$ showing 50% probability ellipsoids and the atom-labeling scheme. Hydrogen atoms have been omitted for clarity.

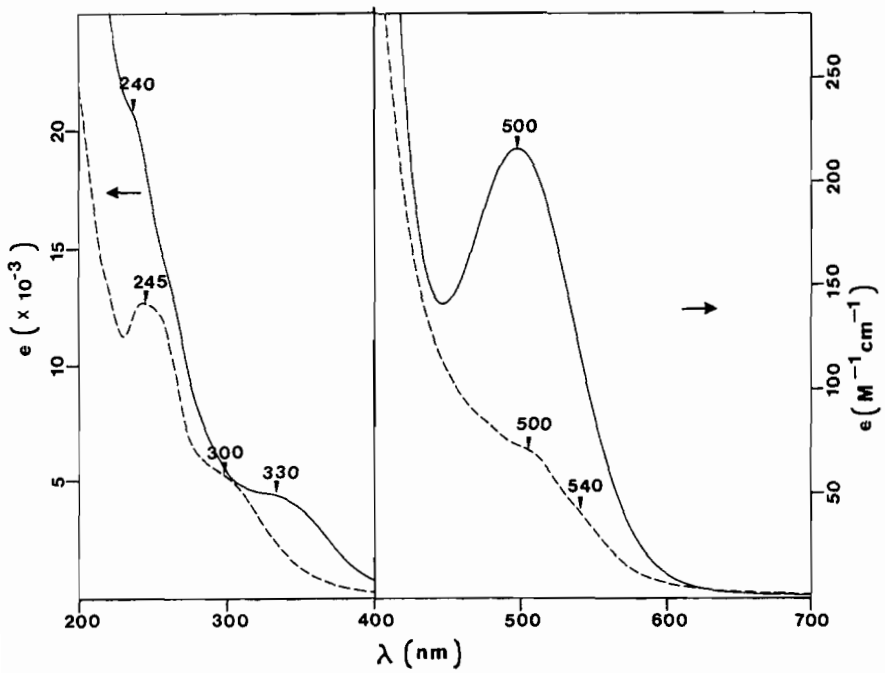

Fig. 2. Absorption spectrum of $[Co(Prpep)_2]ClO_4 \cdot 2.25H_2O$ (**5a**) in methanol (solid line). The 700–200 nm portion of the absorption spectrum of the Co(II) species formed in reaction between 3 and cobalt(II) acetate in methanol under anaerobic condition is shown by the broken line. The latter complex exhibits another band with a maximum at 1070 nm ($\epsilon = 9\ M^{-1}\ cm^{-1}$).

Properties

The dark red color of the $[Co(Prpep)_2]^+$ complex ion arises from a moderately strong band ($\epsilon \sim 200$ $M^{-1}\ cm^{-1}$) around 500 nm (Fig. 2, Table 4). For low-spin octahedral Co(III), two d–d transitions, namely $A_{1g} \rightarrow T_{1g}$ and $^1A_{1g} \rightarrow {}^1T_{2g}$ are expected. The $A_{1g} \rightarrow$

TABLE 4. Spectroscopic data for $[Co(Prpep)_2]ClO_4 \cdot 2.25H_2O$ (5a)[a]

Electronic absorption spectrum	
Solvent	λ_{max} (nm) (ϵ)
Water	490 (200), 325 (4900), 240sh (21000)
MeOH	500 (220), 330 (4800), 240sh (21500)
Me_2SO	506 (245), 345 (4400)

^1H NMR spectrum ($(CD_3)_2SO$, 313 K, δ from TMS)

2.34 (t, J = 12 Hz, 1H), 2.98 (d, J = 15 Hz, 1H), 3.33 (H_2O peak, br), 3.63 (t, J = 12 Hz, 1H), 4.58 (d, J = 15 Hz, 1H), 7.10 (s, 1H), 7.71 (s, 1H), 8.01 (d, J = 5 Hz, 1H), 8.75 (s, 1H), 9.04 (d, J = 5 Hz, 1H), 12.82 (br, 1H).

^{13}C NMR spectrum ($(CD_3)_2SO$, 313 K, δ from TMS)

24.40, 41.82, 115.20, 120.20, 137.14, 137.87, 157.84, 161.39, 161.51, 169.42

[a]Spectral parameters for $[Co(Prpep)_2]BF_4 \cdot 2H_2O$ (5b) are practically identical to that of the perchlorate salt 5a.

$^1T_{1g}$ transition gives rise to an absorption band in the region of 450–500 nm ($\epsilon \sim 10$–300 M^{-1} cm^{-1}) in complexes with the $Co(III)N_6$ chromophore [35] while peptide complexes with the $Co(III)N_4O_2$ chromophore exhibit the same band at ~520 nm ($\epsilon \sim 250$–400 M^{-1} cm^{-1}) [24, 26, 34]. We tentatively assign the 500 nm band of $[Co(Prpep)_2]^+$ to the $^1A_{1g} \rightarrow {}^1T_{1g}$ transition. $[Co(Pypep)_2]^+$ also exhibits the same band at ~500 nm ($\epsilon \sim 200$ M^{-1} cm^{-1}) [18]. The ligand field strength of PrpepH and PypepH thus appears to be very similar. In crystal field of high symmetry, the two d–d transitions in Co(III) complexes give rise to two absorption bands of nearly equal intensity. However, with lowering of symmetry, as is the case with the peptide complexes, the intensity of the band due to $^1A_{1g} \rightarrow {}^1T_{2g}$ transition in the 390–400 region drops. Clearly, the second absorption band of $[Co(Prpep)_2]^+$ around 330 nm (Fig. 2) is too strong for a d–d transition and arises from charge-transfer absorption. Following comparison with $[Fe(Pypep)_2]^+$, the ~330 nm band of $[Co(Pypep)_2]^+$ has been assigned to a ligand-to-metal-charge-transfer (LMCT) transition [18]. The same argument holds good in the present case and hence the ~330 nm band of $[Co(Prpep)_2]^+$ is assumed to be a LMCT band. It is interesting to note that a 324 nm band (ϵ = 6500 M^{-1} cm^{-1}) in the absorption spectrum of the Co(III) complex of the pseudotetrapeptide of BLM has also been suggested to have a charge-transfer origin [10]. Absorption in the ~250 nm region by $[Co(Prpep)_2]^+$ is associated with the organic chromophore(s) of the peptide ligand.

When done under dinitrogen, addition of 1 eq. of cobalt(II) acetate tetrahydrate to 2.1 eq. of 3 in anhydrous methanol produces an orange solution. The electronic spectrum of the orange solution is shown in Fig. 2. Absorption maxima at 1070 (ϵ = 9 M^{-1} cm^{-1}), 540 (ϵ = 40 M^{-1} cm^{-1}), 500 (ϵ = 70 M^{-1} cm^{-1}), 300 (ϵ = 5000 M^{-1} cm^{-1}) and 245 (ϵ = 13 000 M^{-1} cm^{-1}) nm suggest the presence of an octahedral Co(II) species in such a solution [24, 36]. Since no EPR spectrum is observed with the orange solution at liquid nitrogen temperature, a high-spin configuration of the metal center is anticipated [37]. No further characterization of the Co(II) species has been completed at the present time.

The redox properties of $[Co(Prpep)_2]^+$ have been studied by cyclic voltammetry. In solvents like DMF and methanol, $[Co(Prpep)_2]^+$ exhibits a quasireversible one-electron redox process with half-wave potential ($E_{1/2}$) values close to –0.50 V versus SCE. The $E_{1/2}$ values for $[Co(Prpep)_2]^+$ are consistently less negative as compared to those for $[Co(Pypep)_2]^+$. For example in DMF, the $E_{1/2}$ values for $[Co(Prpep)_2]^+$ and $[Co(Pypep)_2]^+$ are –0.50 and –0.70 V (versus SCE), respectively. This suggests that the +3 oxidation state of cobalt is more stabilized by the pyridine based ligand PypepH (2).

Apart from shift in $E_{1/2}$ values, the electrochemical behavior of $[Co(Prpep)_2]^+$ resembles that of $[Co(Pypep)_2]^+$ [18] rather closely. In aprotic solvents like DMF, cyclic voltammograms at slow scan speeds (~50 mV/s) indicate that the Co(II) species generated from one-electron reduction of $[Co(Prpep)_2]^+$ undergoes subsequent reaction or decomposition near the working electrode since a much smaller anodic current is detected in the reverse scan. Variable-scanspeed-voltammetry at glassy carbon electrode reveals that the ratio of cathodic and anodic current (i_c/i_a) approaches the value of 1 at high scan speed (over 200 mV/s). In protic solvents

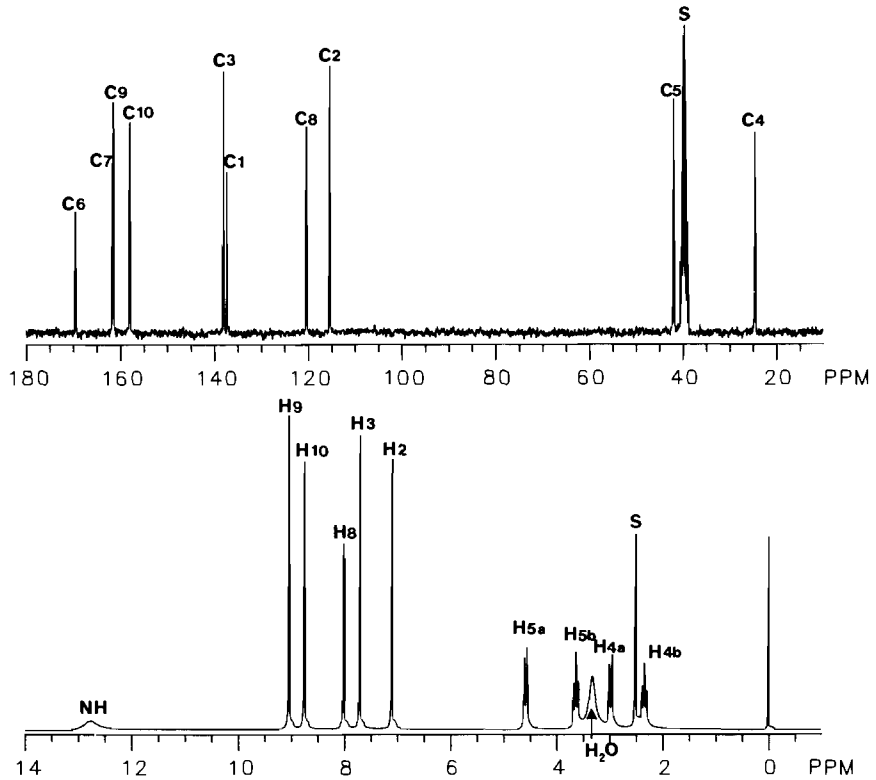

Fig. 3. ^{1}H (lower trace) and ^{13}C (upper trace) NMR spectra (300 MHz, 313 K) of $[Co(Prpep)_2]ClO_4 \cdot 2.25H_2O$ (**5a**) in $(CD_3)_2SO$. Signal assignments (see Fig. 6) are indicated.

like methanol and water, reversibility is not observed even at scan rate of 2 V/s. Since deprotonated amido nitrogen is not a good donor center for Co(II) [25], we believe that the ligand is partially detached from the metal center as $[Co(Prpep)_2]^+$ is reduced. Further changes in the coordination sphere of the labile Co(II) species are also possible. That such processes are indeed taking place in solution is evidenced by the small anodic current noted in the cyclic voltammetric studies. Overall, lability of the Co(II) species generated from simpler analogues like $[Co(Prpep)_2]^+$ (and $[Co(Pypep)_2]^+$ [18]) indicates that precautions must be taken in assigning the solution structure of Co(II)–BLM.

The ^{1}H and ^{13}C NMR spectra of $[Co(Prpep)_2]ClO_4 \cdot 2.25H_2O$ (**5a**) in $(CD_3)_2SO$ are shown in Fig. 3 and the various peak positions are listed in Table 4. In Fig. 3 (and the following Figs.) the hydrogen and carbon atoms of the complex **5a** have been labeled in accordance with Fig. 1 and only the numbers used for one ligand framework are shown, i.e. C4 is also C14, H8 is also H18, etc. The resonances in Fig. 3 have been assigned on the basis of ^{1}H–^{1}H and ^{1}H–^{13}C COSY results (*vide infra*) as well as APT and DEPT data.

The proton resonances for two CH_2 groups of the free ligand **3** appear at 2.82 (a triplet) and 3.60 (a quartet) ppm in its ^{1}H NMR spectrum. $[Co(Prpep)_2]^+$ however, exhibits a doublet-triplet-doublet-triplet (dtdt) pattern in the CH_2 region (1–5 ppm from TMS, Fig. 3), i.e. in the cobalt(III) complex (**5a** or **5b**) the four H atoms are clearly distinguishable and give rise to four different peaks with structures due to mutual couplings. The ^{1}H–^{13}C COSY spectrum (Fig. 5) indicates that each CH_2 group affords a set of one doublet and one triplet while the ^{1}H–^{1}H COSY spectrum (Fig. 4) shows that all four H atoms are coupled to each other. No change in the 'dtdt' pattern is observed with change in temperature in the region of 296–360 K. Clearly, the four H atoms are rigidly held in space in $[Co(Prpep)_2]^+$. The same behavior has been observed with $[Co(Pypep)_2]^+$ [18]. Coupling constant analyses for interactions among the four H atoms in $[Co(Prpep)_2]^+$ have been completed (see 'Supplementary Material'). The water molecules of **5a** resonate at 3.33 ppm (Fig. 3); the peak disappears on addition of D_2O. Resonances for the two imidazole protons H2 and H3 appear at 7.10 and 7.71 ppm, respectively. These assignments rely on the peak positions for the same H atoms in $[Co(Pypep)_2]^+$ [18] and other histidinato [38] and imidazole [31] complexes of tervalent cobalt. The NH peak shifts from 11.15 ppm in **3** to 12.82 ppm in $[Co(Prpep)_2]^+$ following donation of electron density by N1 to the metal center. Similar deshielding of the NH proton has been observed with $[Co(Pypep)_2]^+$. Interestingly,

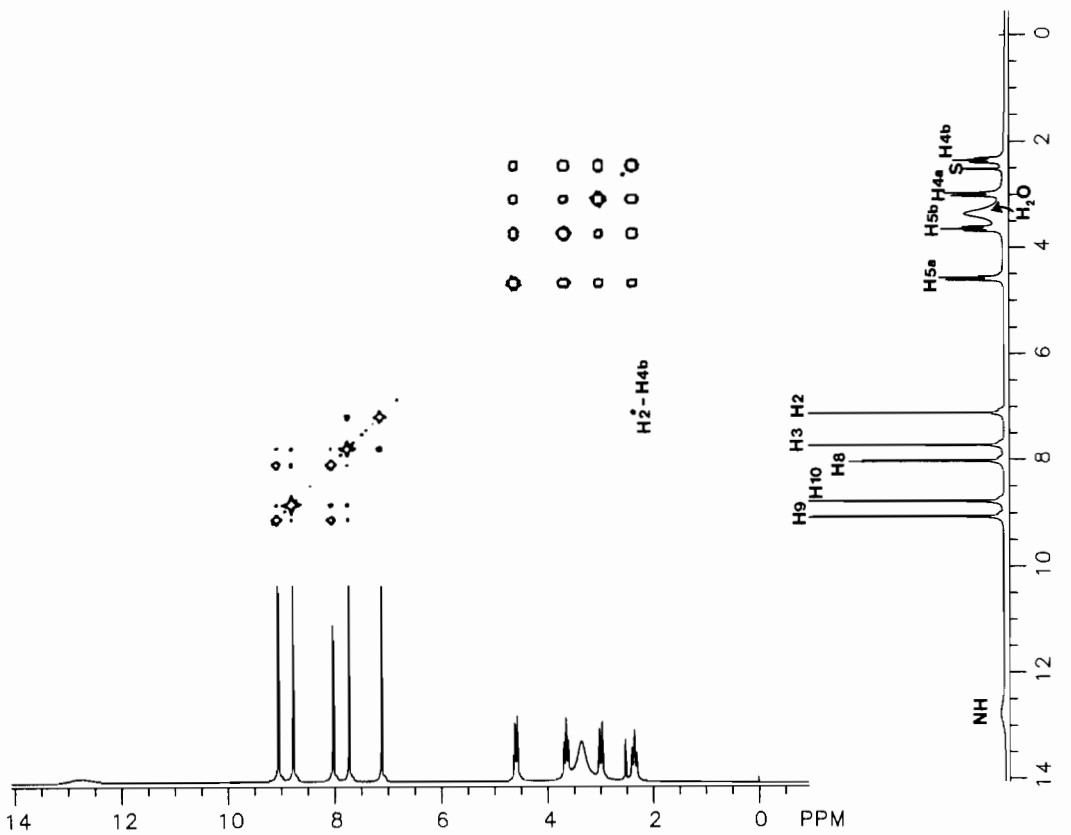

Fig. 4. $^1H-^1H$ COSY spectrum of $[Co(Prpep)_2]ClO_4 \cdot 2.25H_2O$ (**5a**) in $(CD_3)_2SO$.

coordination of N4 of the pyrimidine ring to cobalt results in shielding of H10 and the H10 peak moves from 9.23 ppm in **3** to 8.75 ppm in $[Co(Prpep)_2]^+$. Peak positions for the other pyrimidine ring protons (H8 and H9) have been assigned on the basis of chemical shifts, multiplicities and the values of the coupling constants [39].

Ten distinct resonances for the ten carbon atoms of the ligand are observed in the ^{13}C spectrum of $[Co(Prpep)_2]^+$ (Fig. 3). Assignments of peaks for the quaternary carbons (C1, C6 and C7) and the two CH_2 groups (C4 and C5) rely on APT and DEPT data. The peak corresponding to the carbonyl group (C6) moves from 162.28 ppm in the free ligand (**3**) to 169.44 ppm in the cobalt(III) complex. Downfield shift of the ^{13}C resonance of the carbonyl group due to coordination of the deprotonated amido nitrogen to Co(III) has been observed before [18]. The $^1H-^{13}C$ COSY spectrum of **5a** (Fig. 5) and ref. 39 were used in the assignment of the resonances for the various ring carbons.

Variable temperature ^1H and ^{13}C NMR spectra of $[Co(Prpep)_2]^+$ indicate that in solution the ligand framework remains rather rigid around the metal center. We have therefore added hydrogen atoms to the framework shown in Fig. 1 and have come up with a solution structure of $[Co(Prpep)_2]^+$ which is shown in Fig. 6. This structure is supported by both $^1H-^1H$ and $^1H-^{13}C$ COSY spectra (Figs. 4 and 5). It should be pointed out here that in Fig. 6 we only intend to show the connectivity of the atoms and the relative dispositions of the H atoms; the figure is *not* a result of energy minimization calculation of any kind.

The $^1H-^1H$ COSY spectrum of **5a** (Fig. 4) shows that the H atoms of the two CH_2 groups of the ligand are strongly correlated. It also indicates that H4b is coupled to H2 of the imidazole ring. A *vicinal* coupling constant of 12 Hz allowed us to draw H5b *trans* to H4b. The approximate orientations of the remaining C–H bonds are deduced from *geminal* coupling constant of 14–15Hz and *vicinal* coupling constant of 3–4 Hz (see 'Supplementary Material'). The imidazole protons H2 and H3 are correlated. Unlike $[Co(Pypep)_2]ClO_4 \cdot H_2O$ (**4**) where the water molecule is coupled to the NH group of the imidazole [18], in $[Co(Prpep)_2]ClO_4 \cdot 2.25H_2O$ (**5a**), no correlation between the water molecule(s) and NH group is observed.

The present work provides structural information on a cobalt(III) complex (**5a**) of a peptide ligand PrpepH (**3**) which mimics three of the five proposed donor functionalities of BLM (**1**). Therefore, the structural parameters of **5a** and the NMR assignments

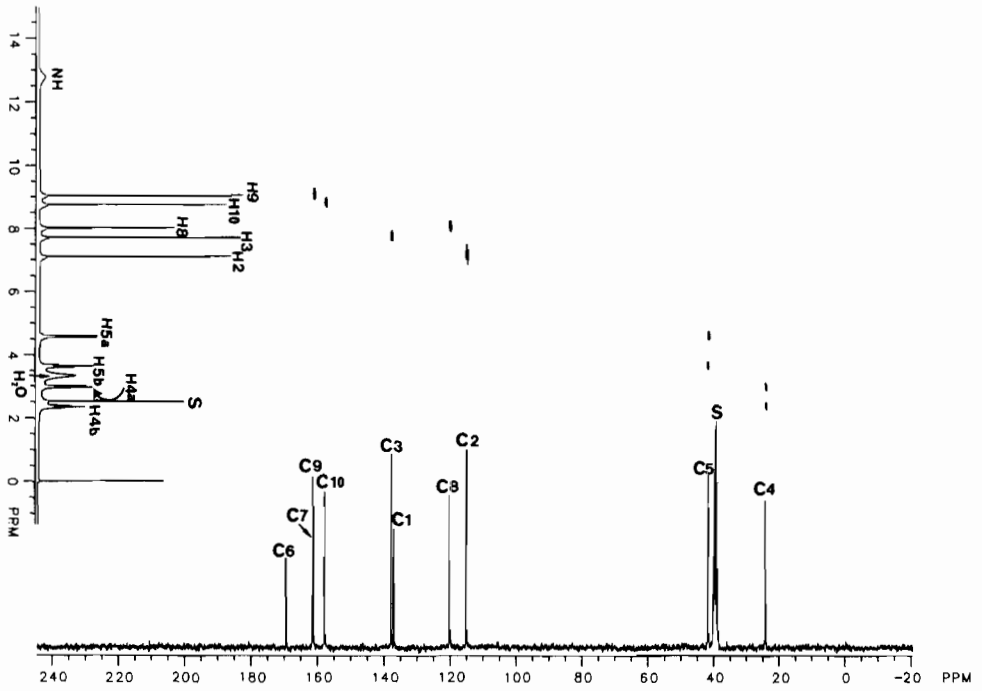

Fig. 5. $^{1}H-^{13}C$ (J = 140 Hz) COSY spectrum of $[Co(Prpep)_2]ClO_4 \cdot 2.25H_2O$ (**5a**) in $(CD_3)_2SO$.

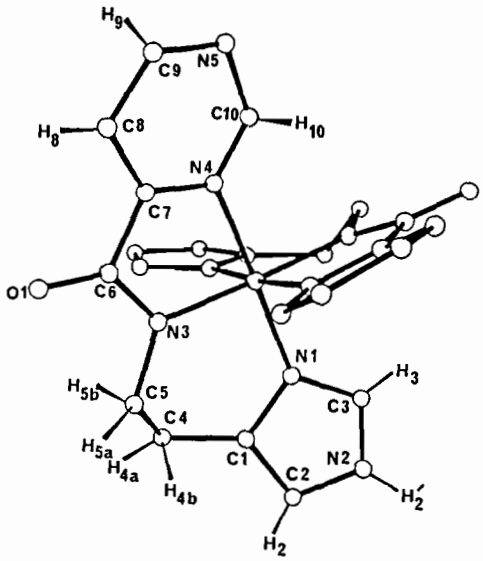

Fig. 6. Proposed solution structure of $[Co(Prpep)_2]ClO_4 \cdot 2.25H_2O$ (**5a**) in $(CD_3)_2SO$ as indicated by the NMR data (see text).

are expected to provide help in elucidation of the coordination structure of Co(III)–BLM.

Supplementary Material

Thermal parameters of the cation (Table S1), positional parameters for hydrogen atoms (Table S2), bond distances and angles involving the H atoms (Table S3) and the structure factor table (Table S4) [total 16 pages]; NMR data for **5a** including coupling constants for the CH_2 protons of the ligand (S5) are available from the authors on request.

Acknowledgements

Support from the donors of the Petroleum Research Fund, administered by the American Chemical Society at the University of California, Santa Cruz and NIH Grant GM 32690 at the University of Texas, Austin is gratefully acknowledged. We thank Steve Brown and Jim Loo for experimental assistance.

References

1 J. Stubbe and J. W. Kozarich, *Chem. Rev., 87* (1987) 1107; S. M. Hecht, *Acc. Chem. Res., 19* (1986) 383.
2 Y. Sugiura, T. Takita and H. Umezawa, *Met. Ions Biol. Syst., 19* (1985) 81.
3 J. C. Dabrowiak, *Adv. Inorg. Biochem., 4* (1983) 69; *Met. Ions Biol. Syst., 11* (1980) 305; *J. Inorg. Biochem., 13* (1980) 317.
4 L. F. Povrick, in S. Neidle and M. J. Waring (eds.), *Molecular Aspects of Anticancer Drug Action*, Macmillan, London, 1983, p. 157.
5 H. Umezawa and T. Takita, *Struct. Bonding (Berlin), 40* (1980) 73.
6 S. M. Hecht (ed.), *Bleomycin: Chemical, Biochemical and Biological Aspects*, Springer, New York, 1979.

7 S. K. Carter, S. T. Crooke and H. Umezawa (eds.), *Bleomycin: Current Status and New Developments*, Academic Press, New York, 1978.
8 E. A. Sausville, J. Peisach and S. B. Horwitz, *Biochemistry, 17* (1978) 2740; K. Nagai, H. Suzuki, N. Tanaka and U. Umezawa, *J. Antibiot., 22* (1969) 569; K. Nagai, H. Yamaki, H. Suzuki, N. Tanaka and H. Umezawa, *Biochim. Biophys. Acta, 179* (1969) 165.
9 Y. Sugiura, *J. Am. Chem. Soc., 102* (1980) 5216; *Biochem. Biophys. Res. Commun., 88* (1979) 913; *J. Antibiot., 31* (1978) 1206.
10 M. Tsukayama, C. R. Randall, F. S. Santillo and J. C. Dabrowiak, *J. Am. Chem. Soc., 103* (1981) 458; J. C. Dabrowiak and M. Tsukayama, *J. Am. Chem. Soc., 103* (1981) 7543.
11 C. M. Vos and G. Westera, *J. Inorg. Biochem., 15* (1981) 253; C. M. Vos, G. Westera and D. Schipper, *J. Inorg. Biochem., 13* (1980) 165; C. M. Vos, G. Westera and B. van Zanten, *J. Inorg. Biochem., 12* (1980) 45.
12 H. Umezawa, T. Takita, Y. Sugiura, M. Otsuka, S. Kobayashi and M. Ohno, *Tetrahedron, 40* (1984) 501; Y. Sugiura, T. Suzuki, M. Otsuka, S. Kobayashi, M. Ohno, T. Takita and H. Umezawa, *J. Biol. Chem., 258* (1983) 1328.
13 J. P. Albertini and A. Garnier-Suillerot, *Biochemistry, 21* (1982) 6777; A. Garnier-Suillerot, J. P. Albertini and L. Tosi, *Biochem. Biophys. Res. Commun., 102* (1981) 499.
14 J. Kakinuma, R. Kagiyama and H. Orii, *Eur. J. Nucl. Med., 5* (1980) 159; P. Raban, J. Brousil and P. Svikovcova, *Eur. J. Nucl. Med., 4* (1979) 191; L. H. DeRiemer, C. F. Meares, D. A. Goodwin and C. I. Diamanti, *J. Med. Chem., 22* (1979) 1019; A. Kono, Y. Matsushima, M. Kojima and T. Maeda, *Chem. Pharm. Bull., 25* (1977) 1725; A. D. Nunn, *Intl. J. Nucl. Med. Biol., 4* (1977) 204; J. P. Nouel, *Gann Monogr. Cancer Res., 19* (1976) 301; J. J. Rasker, M. A. P. C. Van de Poll, H. Beekhins, M. G. Woldring and H. O. Nieweg, *J. Nucl. Med., 16* (1975) 1058.
15 C. H. Chang, L. L. Dallas and C. F. Meares, *Biochem. Biophys. Res. Commun., 110* (1983) 959.
16 C. H. Chang and C. F. Meares, *Biochemistry, 23* (1984) 2268; *21* (1982) 6332.
17 J. A. Ibers and R. H. Holm, *Science (Washington, D.C.), 209* (1980) 223.
18 K. Delany, S. K. Arora and P. K. Mascharak, *Inorg. Chem., 27* (1988) 705.
19 S. J. Brown, X. Tao, T. A. Wark, D. W. Stephan and P. K. Mascharak, *Inorg. Chem., 27* (1988) 1581; S. J. Brown, X. Tao, D. W. Stephan and P. K. Mascharak, *Inorg. Chem., 25* (1986) 3377.
20 G. A. Archer, R. I. Kalish, R. Y. Ning, B. C. Sluboski, A. Stemple, T. V. Steppe and L. H. Sternbach, *J. Med. Chem., 20* (1977) 1312.
21 R. Benn and H. Gunther, *Angew. Chem., Int. Ed. Engl., 48* (1983) 350.
22 G. M. Sheldrick, *SHELX-76*, program for crystal structure determination, University of Cambridge, Cambridge, 1976.
23 D. T. Cromer and J. T. Weber, in *International Tables for X-ray Crystallography*, Vol. IV, Kynoch Press, Birmingham, U.K., 1974.
24 P. J. Morris and R. B. Martin, *Inorg. Chem., 10* (1971) 964.
25 H. Sigel and R. B. Martin, *Chem. Rev., 82* (1982) 385.
26 L. V. Boas, C. A. Evans, R. D. Gillard, P. R. Mitchell and D. A. Phipps, *J. Chem. Soc., Dalton Trans.*, (1979) 528.
27 F. A. Cotton and G. Wilkinson, in *Advanced Inorganic Chemistry*, Wiley, New York, 5th edn., 1988, pp. 735–738.
28 B. A. Cartwright, P. O. Langguth, Jr. and A. C. Skapski, *Acta Crystallogr., Sect. B, 35* (1979) 63; B. A. Cartwright, D. M. L. Goodgame, I. Jeeves, P. O. Langguth Jr. and A. C. Skapski, *Inorg. Chim. Acta, 24* (1977) L45.
29 T. J. Kistenmacher, T. Sorrell, M. Rossi, C. C. Chiang and L. G. Marzilli, *Inorg. Chem., 17* (1978) 479.
30 R. Herak, B. Prelesnik, B. Kamberi and M. B. Celap, *Acta Crystallogr., Sect. B, 37* (1981) 1989.
31 N. R. Brodsky, N. M. Nguyen, N. S. Rowan, C. B. Storm, R. J. Butcher and E. Sinn, *Inorg. Chem., 23* (1984) 891.
32 R. D. Gillard, E. D. McKenzie, R. Mason and G. B. Robertson, *Nature (London), 209* (1966) 1347.
33 M. T. Barnet, H. C. Freeman, D. A. Buckingham, I. Hsu and D. van der Helm, *J. Chem. Soc., Chem. Commun.*, (1970) 367.
34 J. E. Evans, C. J. Hawkins, J. Rodgers and M. R. Snow, *Inorg. Chem., 22* (1983) 34.
35 A. B. P. Lever, in *Inorganic Electronic Spectroscopy*, Elsevier, Amsterdam, 2nd edn., 1984, pp. 463–478.
36 A. B. P. Lever, in *Inorganic Electronic Spectroscopy*, Elsevier, Amsterdam, 2nd edn., 1984, pp. 480–489.
37 R. S. Drago, in *Physical Methods in Chemistry*, Saunders, Philadelphia, 1977, Ch. XIII, p. 497.
38 C. J. Hawkins and J. Martin, *Inorg. Chem., 25* (1986) 2146.
39 K. Biemann, in *Tables of Spectral Data for Structure Determination of Organic Compounds*, Springer, West Berlin, 1983 (translated from German).